# Effect of strongly anharmonic longitudinal and transverse vibrations with wave vector k=2/3(111) on the structural stability of β-Zr under pressure

V. Yu. Trubitsin*
*Physico-Technical Institute, Ural Branch of RAS, 132 Kirov Strasse, 426001 Izhevsk, Russia*
(Received 16 December 2005; published 16 June 2006)

The pressure and temperature dependence of the vibrational frequency of two interacting strongly anharmonic longitudinal and transverse modes with wave vector $\mathbf{k}=2/3(111)$ in $\beta$-Zr is studied by solving a set of stochastic differential Langevin equations with a thermostat of the white noise type. The appropriate effective potential is calculated within the electron density functional theory, taking into account the contributions to the free energy from the electronic entropy depending on the atomic displacements. An analysis of the changes in the spectral density of vibrations with the pressure and temperature allows us to determine the stability region of the bcc phase of zirconium at pressures up to 35 GPa. A good agreement is obtained with the experimental data available. From the calculation performed it follows that the structural instability of the Zr bcc lattice with respect to the displacements characteristic of vibrations with wave vector $\mathbf{k}=2/3(111)$ is of significant importance not only for the $\beta\rightarrow\omega$ transition, but also for the $\beta\rightarrow\alpha$ transformation observed at pressures less than 5 GPa.

DOI: 10.1103/PhysRevB.73.214303 PACS number(s): 63.20.Ry, 05.10.Gg, 63.20.Kr, 71.15.Nc

## I. INTRODUCTION

In the preceding paper[1] we have studied the effect of the temperature on the effective potential $W(x,y)$ and spectral density of vibrations of the interacting longitudinal, $x$, and transverse, $y$, modes with wave vector $\mathbf{k}=2/3(111)$ ($L_l$ and $L_t$ phonons). The effective potential acting on these modes at zero temperature was calculated in the frozen-phonon approximation within the framework of the electron density functional theory by the FP LMTO method.[2,3] For nonzero temperatures, the $W_T$ potential was defined as the difference in free energy $F_T$ for different atomic displacements, $W_T(x,y)=F_T(x,y)-F_T(0,0)$. We have shown that the shape of the effective potential is essentially temperature dependent. An analysis of the changes with temperature in the frequency dependence of the transverse $L_t$ vibrations allowed the stability region of the Zr $\beta$ phase to be determined at zero pressure.

It is currently believed that, at atmospheric pressure, the low-temperature instability of $\beta$-Zr is due to the softening of the transverse phonon with wave vector $\mathbf{k}=1/2(110)$ ($N_t$ phonon).[4–6] The result we obtained[1] testifies that at zero pressure there is, at least, one more process responsible for the structural instability of the Zr bcc lattice, namely, the atomic displacements corresponding to the longitudinal $L_l$ phonon. This phonon mode is commonly associated with the $\beta\rightarrow\omega$ transformation observed in zirconium at high pressures.[7,8] We have shown[1] that for $P=0$ GPa the temperature at which the $\beta$ phase of Zr becomes unstable to the longitudinal $L_l$ displacements is $T_L=1150\pm50$ K. This value practically coincides with the experimentally obtained $\beta\rightarrow\alpha$ transition temperature $T_{\beta\rightarrow\alpha}=1136$ K.[9] The question now arises of whether the close agreement between $T_L$ and $T_{\beta\rightarrow\alpha}$ is accidental or the $L_l$ mode plays really an important, if not decisive, role in the $\beta\rightarrow\alpha$ transformation. To answer this question one should determine the region of stability of bcc Zr with respect to the atomic displacements characteristic of the $L_l$ mode at different pressures.

Earlier, we have shown[6] that with increasing pressure the temperature of the transition due to the $N_t$ mode softening must decrease. In the present paper, using the approach developed in Ref. 1, we shall calculate the changes with the pressure in the spectral density of the longitudinal, $L_l$, and transverse, $L_t$, modes with wave vector $\mathbf{k}=2/3(111)$, and determine, in a wide temperature and pressure range, the stability region of the Zr $\beta$ phase with respect to the displacements corresponding to these modes. To this end, we shall successively consider the dependence on the volume, $V$, and atomic displacements, $x,y$, of the total energy of a crystal in the ground state, $E^V_{\mathrm{el}}(x,y)$ (2D analog of the frozen-phonon model), electronic entropy $S^V_{\mathrm{el}}(T,x,y)$ and free energy

$$F^V_T(x,y)=E^V_{\mathrm{el}}(x,y)-TS^V_{\mathrm{el}}(T,x,y). \quad (1)$$

The effective potentials $W_T(x,y)=F_T(x,y)-F_T(0,0)$ calculated for each fixed volume and temperature will be used in solving a set of stochastic differential equations of motion with a thermostat of the white noise type.

A similar stochastic approach to modeling the lattice vibrations of a strongly anharmonic crystal (including the $L_l$ mode of Zr) was used in Ref. 10 where, in contrast to this paper, the dynamics of motion of *a single mode in a temperature-independent potential were studied at zero pressure*.

## II. DETAILS OF CALCULATION

As in Ref. 1, the unit cell of $\beta$-Zr was chosen as a hexagonal lattice with three base atoms. A detailed description of the unit cell geometry, its relation with the bcc lattice parameters, and the atomic displacements corresponding to the vibrations with the chosen wave vector $\mathbf{k}=2/3[111]$ may be found, for example, in Ref. 11. The total energy was calculated by the self-consistent full-potential LMTO method (FP LMTO) (Refs. 2 and 3) with the GGA approximation for the exchange-correlation potential term.[12] The same set of FP

 

LMTO parameters was used for all displacements. The one-center expansions inside the MT spheres were confined to $l_{\max}=6$. The MT sphere radii were chosen equal to $R_{mt}=2.20$ a.u. Integration over $k$ was performed on a (10,10,10) mesh equivalent to 166 $k$-points in the irreducible part of the Brillouin zone. The total energy was calculated for 108 pairs of coordinates $x,y$ (18 values for the variable $x$ corresponding to the longitudinal $L_l$ mode, and six values for $y$ corresponding to the transverse $L_t$ mode). The energies obtained were first approximated by a tenth-degree polynomial for the longitudinal vibrations and then by a fourth-degree polynomial for the transverse ones.

The electronic excitation entropy term was introduced as earlier.[1,13] This means that our analysis was limited to the classical lattice-dynamics regime when the electron-phonon interaction effects become negligible and the electronic excitation entropy term $S_{\rm el}$ is bare electronic entropy

$$S_e = -k_B \int n[f \ln f - (1-f)\ln(1-f)]dE. \tag{2}$$

Here $n(E)$ is the density of states, and $f(E)$ is the Fermi distribution

$$f(E) = [\exp \beta(E-\mu) + 1]^{-1}, \tag{3}$$

$\beta=1/(k_BT)$. The chemical potential $\mu(T)$ was determined from the condition for the number of electrons, $z$

$$z = \int n(E)f(E)dE. \tag{4}$$

The obtained temperature-dependent effective potential $W_T^V(x,y)$ was used in solving the set of stochastic differential Langevin-type equations,

$$\frac{d^2x}{dt^2} + \frac{\partial W(x,y)}{\partial x} + \gamma_x \frac{dx}{dt} = F_x(t),$$

$$\frac{d^2y}{dt^2} + \frac{\partial W(x,y)}{\partial y} + \gamma_y \frac{dy}{dt} = F_y(t), \tag{5}$$

$F_x(t)$, $F_y(t)$ are random forces with correlators

$$\langle F_i(t)\rangle = 0, \tag{6}$$

$$\langle F_i(t)F_j(t')\rangle = 2T\gamma\delta_{ij}\delta(t-t'), \tag{7}$$

$\gamma$ are coefficients of the vibration damping, $T$ is the temperature of the thermostat. The set of equations (5) was solved by numerical integration of stochastic differential equations, using a method,[14] which is a generalization of the Runge-Kutta scheme to the stochastic differential equations. We used a four-step method of third order with the parameters from Ref. 14.

When solving the set of stochastic differential equations, a particular effective potential $W(T)$ was constructed for each fixed temperature $T$ in (7). The calculation was performed with a time step $\Delta t=1.57\times10^{-16}$ s, the number of steps in the realization being $N_{sh}=3\times10^8$. Thus, the total time of modeling was $t_r\approx5\times10^{-8}$ s, which is vastly greater than the period of vibrations of the chosen modes. The test calculations for $N_{sh}=9\times10^8$ have shown that the result remains unchanged with such an increase of the modeling time.

The stochastic dynamical variables (coordinates $X,Y$ and velocities $V_X,V_Y$) found by solving Eqs. (5) were used to calculate the autocorrelation velocity functions $\mathbb{K}_i(\tau)=\langle V_i(0)V_i(\tau)\rangle$. To this end the whole interval of modeling time was divided into realizations. The values of dynamical variables $X(t_0),Y(t_0)$ obtained at the end of each realization were used as the starting values for the next one. In the average, the length of one realization was $N_r=100\,000$ steps ($1.57\times10^{-11}$ s). When calculating the correlators, the total number of realizations over which the averaging was performed amounted to 3000.

The spectral vibration density $S_i(\omega)$ was found from the autocorrelation velocity function $\mathbb{K}_i(\tau)$,

$$S_i(\omega) = \frac{2}{\pi}\int_0^\infty \cos(\omega\tau)\mathbb{K}_i(\tau)d\tau. \tag{8}$$

The computational details as well as the effect of the calculation parameters on the result were discussed in Ref. 1.

## III. VOLUME DEPENDENCE OF THE EFFECTIVE POTENTIAL AND SPECTRAL DENSITY OF VIBRATIONS

The effective potential $W(x,0)$ for the longitudinal displacements $L_l$, calculated at different temperatures and four values of the volume ($V=V_0, V=0.9V_0, V=0.8V_0, V=0.7V_0$, here $V_0$ is the equilibrium volume), is shown in Fig. 1. It can be seen that the effective potential for the longitudinal vibrations and equilibrium volume $V=V_0$ has a three-well shape, which agrees with the findings of Ref. 11. The free energy is minimum at zero displacements when the atoms are localized at the sites of the crystalline structure of $\omega$-Zr. Two local minima at $x\approx|0.166|$ correspond to the atomic arrangement in the bcc structure. Because of these minima being shallow, the bcc lattice of zirconium proves to be unstable to small longitudinal vibrations at $V_0$. It should be noted that to obtain the $\omega$ structure observed in Zr from the bcc lattice, it will not suffice to merely shift the atoms, it is also necessary to increase the $c/a$ ratio. In further discussion, we shall not take into account the change of $c/a$ under the $\beta\rightarrow\omega$ structural transformation.

The change of the potential with reduction in the volume qualitatively agrees with the change it undergoes as the temperature increases. First, with small changes in the volume ($V=0.9V_0$), the difference in energy between the bcc and $\omega$ structures diminishes. Then, at $V=0.8V_0$, a plateau appears near the equilibrium position of the $\omega$ structure, i.e., the crystal energy remains almost unchanged at small atomic displacements. For this volume the bcc structure becomes energetically preferential. With further reduction in the volume ($V=0.7V_0$) the effective potential transforms into a two-well one. As a result, the $\omega$ phase becomes unstable with respect to infinitesimal atomic displacements and, hence, only zirconium with a bcc lattice may be stable at $V=0.7V_0$. Note that in spite of qualitatively similar changes of the effective potential with a reduction in the volume and with an increase in temperature, the causes of these changes are completely dif-

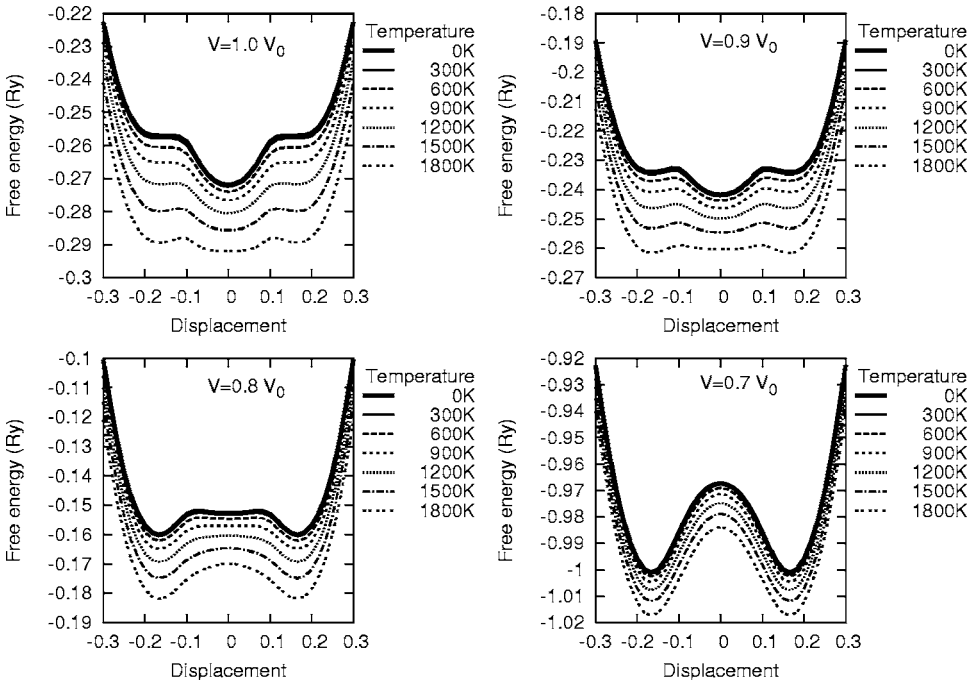


FIG. 1. The effective potential $W(x,0)$ for different temperatures and crystal volumes.

ferent. So, the changes in the potential with increasing temperature are entirely due to the change of the electronic entropy, whereas with reduction in the volume, the change of $W$ is totally caused by the change of the electron structure in the *ground state*. In Fig. 1 we present only the effective potential for the longitudinal atomic displacements, for the transverse ones it has a parabolic shape at both the $\omega$ $[W(0,y)]$ and bcc $[W(0.166,y)]$ sites. We do not show here a three-dimensional (3D) picture of the potential because of its being a little informative and hardly comprehensible. Three-dimensional pictures of the effective potential at different temperatures can be found in Ref. 1, as well as a detailed discussion of the temperature dependence of the potential at a constant volume, $V_0$.

The spectral densities of vibrations, $S_i(\omega)$, are presented in Fig. 2 for different temperatures and volumes. As was shown in Ref. 1, the first maximum of the spectral density $S_x(\omega)$ at low frequencies ($\omega \approx 1.5$ GHz) is associated with the longitudinal vibrations; the second one, at $\omega > 3$ GHz, yields the spectral density of the transverse vibrations, $S_y(\omega)$. As seen, the changes of the spectral density with temperature at $V=0.90V_0$ coincide, on the whole, with those at the equilibrium volume. This is not surprising, since in both cases the effective potential has the same shape, and differs only in the depth of the potential well (see Fig. 1).

It can be seen from the figure that the volume dependence of the vibrational frequency differs for the longitudinal and transverse modes. So, at low temperatures, with a reduction in the volume the frequency decreases for the longitudinal vibrations and increases for the transverse ones. At high temperatures, the frequency of the longitudinal vibrations changes only slightly with reduced volume, and the transverse vibrations frequency increases from $\omega \approx 3.9$ THz for the equilibrium volume up to $\omega \approx 4.5$ THz for $V=0.9V_0$.

It is easily seen from Fig. 2 that with a reduction in the volume, there is a decrease in the temperature at which two equal in intensity peaks appear in the spectral density curve in the region of both longitudinal and transverse vibrations. In Ref. 1 we have shown that the appearance of a double-hump structure in the spectral density curve points to the occurrence of structural instability connected with the given type of vibrations. For the transverse mode, the temperature, at which the spectral density has two equal in intensity peaks, is $T \approx 1200$ K and $T \approx 900$ K for the equilibrium ($V_0$) and reduced $V=0.90V_0$ volume, respectively. For the longitudinal vibrations this temperature is somewhat lower, $T=700$ K and $T=500$ K at the equilibrium and reduced volume.

The appearance of a double peak in the spectral density $S_x(\omega)$ is due to the presence of longitudinal vibrations with energies smaller and greater than the height of the barrier that separates the bcc and $\omega$ phases (see Fig. 1). Similar intensities of the vibration density testify that the share of vibrations higher in energy than the barrier (over-barrier trajectories) is equal to the share of vibrations with an energy lower than the barrier height (vibrations near the $\omega$ center). However, the presence of over-barrier vibrations yields no direct information about the relative portion of time spent by the system, respectively, in the bcc and the $\omega$ phase. As was shown,[1] this information may be extracted from the spectral density of the transverse vibrations, since their frequency directly depends on where the system spends most of the time: near the bcc or the $\omega$ center. Thus, analysis of the spectral density of the transverse vibrations makes it possible to estimate the temperature at which the probability of finding the system in either phase is the same.

In the third panel of Fig. 2 is shown the spectral density of vibrations under a crystal compression to $V=0.80V_0$. On the whole, the changes with temperature in the spectral density $S_x$ coincide, at this volume, with the above-considered case. The main distinction reduces to the presence, at high temperatures of an additional peak in the region of $\omega \approx 2$ THz. At low temperatures ($T<600$ K) this peak is the main one,

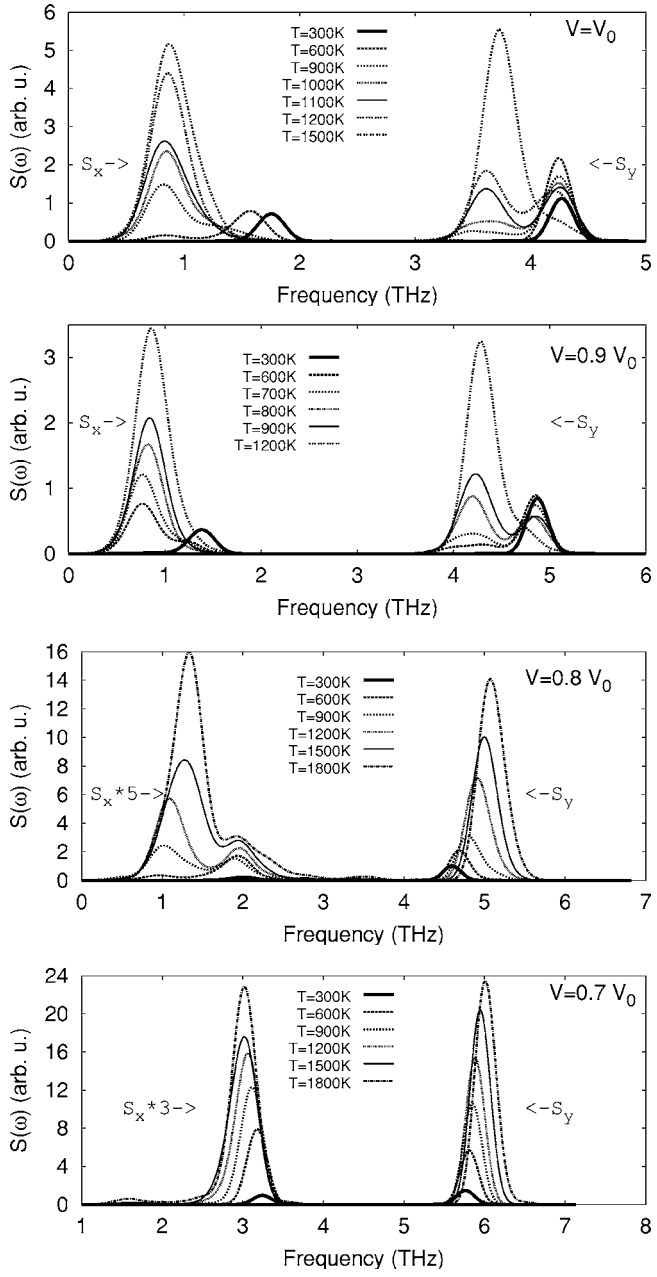


FIG. 2. The spectral density of vibrations for different temperatures and crystal volumes.

and its position remains almost unchanged at all temperatures considered. Despite the apparent resemblance of the spectral density of the $L_l$ mode at $V=0.80V_0$ and $V=V_0$, the lattice dynamics in these cases are quite different. Namely, at the equilibrium volume, $V_0$, the vibrations at low temperatures occur near the $\omega$ sites, while at $V=0.80V_0$ the peak in the frequency range of $\omega \approx 2$ THz is connected with the vibrations near the bcc sites. This is due to the fact that at $V=0.8V_0$ the free energy of the bcc phase is less than the energy of the $\omega$ phase (see Fig. 1) and, hence, at low temperatures the system spends most of the time near the bcc sites ($x \approx 0.16$). With increasing temperature, there appear over-barrier vibrations with a lower frequency, which results in the formation of a $S_y(\omega)$ peak in the frequency range of $\omega \approx 1$ THz. As already noted, the presence of over-barrier trajectories yields no information on the lattice stability.

As seen in Fig. 2, at $V=0.80V_0$, with increasing temperature the maximum of the spectral density of the transverse vibrations shifts slightly to higher frequencies, and a second peak is entirely absent in the $S_y(\omega)$ curve. Such a character of the spectral density change with temperature indicates that, at all temperatures considered, the transverse vibrations are mainly localized near the sites corresponding to the bcc structure. In other words, at this volume the bcc lattice remains stable at any temperature. This can be seen in Fig. 3 which shows the probability density of the longitudinal atomic displacements at different temperatures and crystal volumes.

As follows from the figure, at $V=0.80V_0$, the probability of finding the system near the bcc sites is greater. Nonetheless, at high temperatures, the system still spends much of the time near the $\omega$ sites ($x=0$). Further reduction of the volume to $V=0.70V_0$ causes the vibrations to occur only near the bcc sites. This is completely determined by the shape of the effective potential at this volume (see Fig. 1) and the absence of over-barrier vibrations. Correspondingly, in the spectral density curves at $V=0.70V_0$ (Fig. 2) a second peak does not appear for both the longitudinal and transverse vibrations. With increasing temperature, only a shift of the maxima is observed and, hence, at all temperatures considered, the bcc phase of zirconium is stable.

## IV. TEMPERATURE DEPENDENCE OF THE VIBRATIONS FREQUENCY OF THE $L_t$ MODE OF bcc ZIRCONIUM AND THE *P-T* PHASE DIAGRAM

As has been shown in the preceding section, the relative intensity of the spectral density of the transverse vibrations may be used to estimate the probability of finding the system in one phase or another. The vibration frequencies $\omega_{\max}$ of the transverse $L_t$ mode, for which the spectral density $S_y(\omega)$ reaches its absolute maximum at a given temperature, are shown in Fig. 4. As seen, for $V/V_0 > 0.85$, a slight decrease in $\omega_{\max}$ is observed with increasing temperature. Then, at a certain temperature $T_{tr}$, the vibrational frequency $\omega_{\max}$ sharply decreases. Further increase in temperature causes the frequency of the $L_t$ vibrations to increase. An analysis of the spectral density of transverse vibrations shows that the temperature ranges with higher frequencies correspond to the $\omega$, and those with lower frequencies to the bcc lattice. Since Fig. 4 presents the frequencies at which the spectral density of the transverse vibrations is maximum, a jump in $\omega_{\max}$ occurs at temperatures, for which $S_y(\omega)$ (Fig. 2) has two peaks equal in intensity. In this case the temperature $T_{tr}$ can beconsidered as the $\omega \rightarrow \beta$ phase transition temperature at a constant volume. In the figure, the vertical dotted lines mark the temperature at which there is a sharp change in the transverse vibrations frequency $\omega_{\max}$ for different volumes. As seen, with reduction in the volume the value of $T_{tr}$ diminishes. For $V/V_0 < 0.80$ the frequency $\omega_{\max}$ monotonically increases with temperature, in complete agreement with Fig. 2. Such a behavior indicates that, for the considered volumes, the bcc structure remains stable at all temperatures, and the

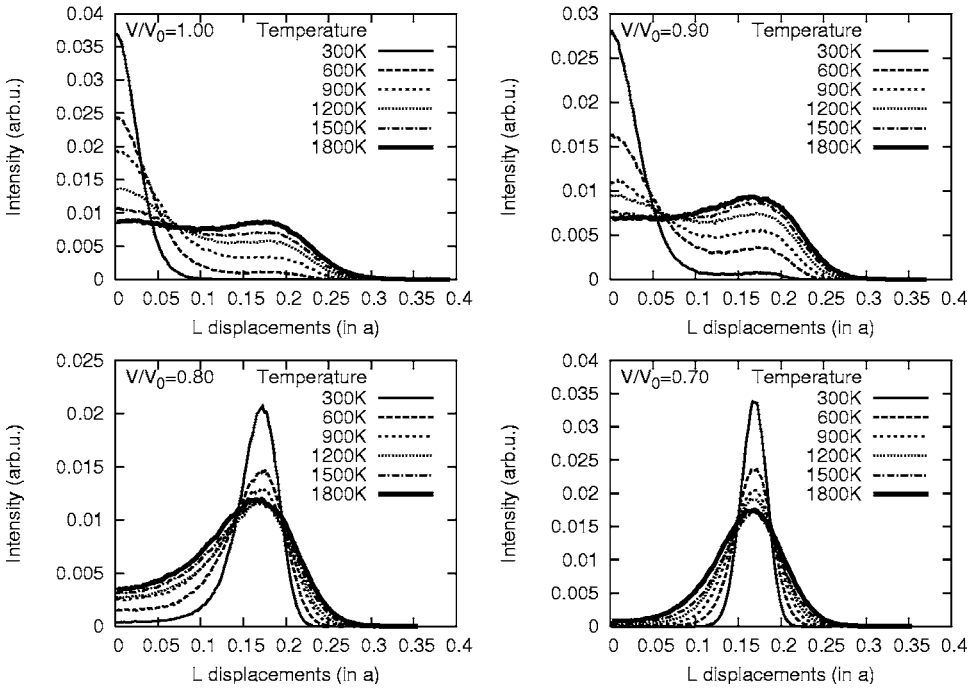


FIG. 3. The probability density of the mean-square displacement for the $L_l$ vibrations at different temperatures and volumes.

structural phase transition connected with this mode does not occur.

Using the values of $T_{tr}$ found in such a way for different $V/V_0$ and the pressure dependence of the volume, $P(V)$ (Fig. 5), calculated within the electron density functional theory, one can determine the stability region of the bcc phase of Zr in the $P$-$T$ plane. In Fig. 6 the obtained values of $T_{tr}, P_{tr}$ are shown by open circles. The solid circles correspond to the known experimental data.[9,16–18] The dotted lines are drawn through the experimental points in order to schematically separate different phases of zirconium, and the solid line indicates the interfaces obtained within the electron density functional theory and the Debye-Grüneisen model.[15]

It can be seen that at small pressures ($P<5$ GPa) the calculated temperature, at which the bcc lattice becomes stable with respect to the atomic displacements corresponding to the $L$ phonon, agrees well with the experimentally measured temperature of the $\beta \rightarrow \alpha$ transition. For example, at atmospheric pressure this temperature is $T=1136$ K.[9] Our calculation yields, at $P=0$ GPa, a value of $T=1150\pm50$ K for the stability boundary of bcc Zr. The triple point found in Ref. 18 has the following coordinates: $P=5.5$ GPa, $T=995$ K. We have obtained, at a pressure $P=5.0$ GPa, a transition temperature value of $1025\pm50$ K. In Ref. 18 the temperatures of the $\beta \rightarrow \alpha$ and $\alpha \rightarrow \beta$ transitions were thoroughly measured at pressures ranging from 1 to 5 GPa. The experimental points obtained are fairly well approximated by a straight line with a slope equal to $-2.4$ °C/kbar. In our calculation, in this interval of pressures there are only two points at 0 and 5 GPa. The slope of the straight line drawn through these points amounts to $-2.5$ °C/kbar, which is in excellent agreement with the experimental values.

Our calculation suggests that in the range of high pressures at room temperature, the bcc lattice becomes stable at 25 GPa. Experimentally, at room temperatures the $\omega \rightarrow$ bcc transition is observed at $30\pm2$ GPa (Ref. 16) and 35 GPa.[17] If it is remembered that our calculation has no fitting parameters, such a result may be considered as quite satisfactory. Unfortunately, no detailed experimental studies of the equi-

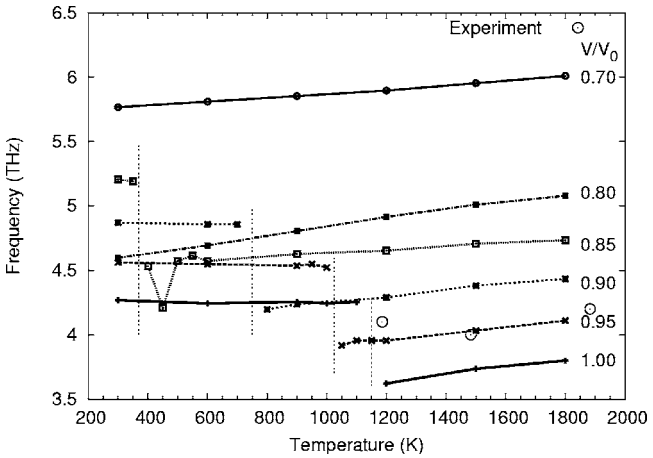


FIG. 4. The frequency $\omega_{\max}$ of the transverse $L_t$ vibrations as a function of temperature for different volumes.

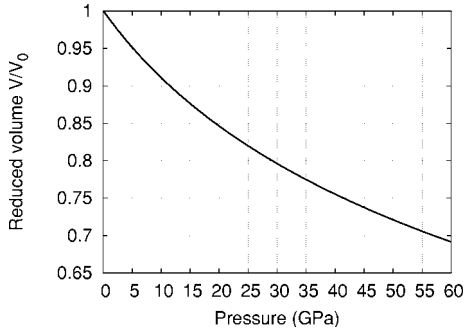


FIG. 5. The equation of state of bcc zirconium calculated within the electron density functional theory.

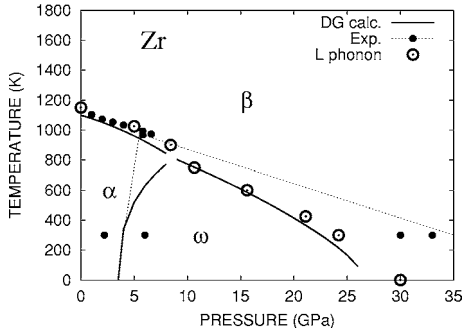


FIG. 6. The $P$-$T$ phase diagram of zirconium: ●, experiment (Refs. 9, 16, and 17); ○, $T_{tr}$ calculation; Debye-Grüneisen calculation (Ref. 15) (solid line).

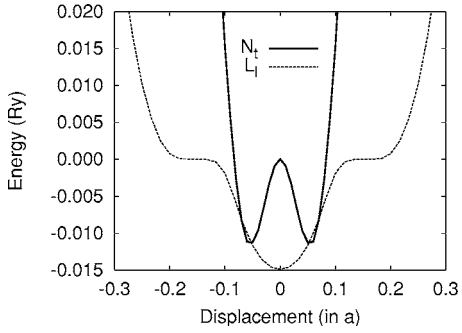


FIG. 7. The effective potential for the transverse ($N_t$) and longitudinal ($L_l$) modes in $\beta$-Zr calculated in the frozen-phonon model.

librium line between the $\omega$ and $\beta$ phases of Zr are currently available. So, in Fig. 6 is also presented the Zr phase diagram we have calculated in the Debye-Grüneisen model[15] (solid line). As seen, there is a quite reasonable agreement between two theoretical calculations performed within different models. Note that in the Debye-Grüneisen model, at $T=300$ K, the $\omega \rightarrow$ bcc transition takes place at a pressure of about 24 GPa, which closely agrees with the value obtained in this work. There may be two main reasons for the discrepancy between theory and experiment observed in the high-pressure range. First, in our calculation the variation of the $c/a$ ratio in the $\omega$ phase with the volume and temperature was not taken into account. Second, the calculation was performed for an ideal structure, whereas experimentally, it is not feasible to obtain a perfect crystal under pressure.

As we have repeatedly noted, the displacements corresponding to the $L$ mode result in the formation of a hexagonal $\omega$ lattice. At the same time, at $P<5.0$ the formation of a hcp lattice ($\alpha$ phase) is experimentally observed with decreasing temperature. The $\beta \rightarrow \alpha$ structural phase transition in Zr is usually attributed to an anomalous softening of the transverse phonon at the $N$ point of the Brillouin zone of the bcc lattice. We have calculated[6] the effective potential of the $N$ phonon of Zr at different volumes. An analysis of the changes in the potential shape with the pressure allows us to conclude that with increasing pressure the temperature at which the bcc lattice becomes unstable with respect to the $N$ phonon diminishes. Thus, in the pressure range from 0 to 5 GPa and the temperature interval from 1000 to 1200 K there exist at least two competitive processes responsible for the disturbance of stability of the Zr bcc lattice.

The effective potentials of the transverse, $N_t$,[19] and longitudinal, $L_l$, modes in $\beta$-Zr calculated in the frozen-phonon model are shown in Fig. 7. The energy of the bcc phase was chosen as the zero of energy. The zero on the abscissa corresponds to the bcc structure for the $N_t$ mode, and for the $L_l$ mode, as before, to the $\omega$ structure. For the $N_t$ phonon the effective potential has a double-well shape with a central energy maximum corresponding to the bcc structure. Such a shape of the potential results in the fact that, at low temperatures, the bcc lattice becomes unstable with respect to the displacements corresponding to the $N_t$ phonon. With increasing temperature, when the energy of the system exceeds the barrier height, stabilization of the bcc structure is likely to occur. Since the barrier height for the $N_t$ phonon is less than for the $L_l$ one, the temperature, at which the bcc lattice of Zr becomes unstable with respect to the atomic displacements corresponding to the $N_t$ mode, should be lower than for the $L_l$ mode.

If these are realistic assumptions, the following scenario of the $\beta \rightarrow \alpha$ phase transition could be expected: with decreasing temperature, in $\beta$-Zr there first arises instability with respect to the $L_l$ vibrations, which results in the formation of a metastable $\omega$ phase. Since the $\omega$ phase is unstable in this range of temperatures and pressures, it transforms, in a short time, into an $\alpha$ phase. At pressures above the triple point, the $\omega$ phase becomes stable and its transition into the $\alpha$ phase with a hcp lattice does not occur.

It is not our intention, in this paper, to prove or disprove such a plausible scenario for the $\beta \rightarrow \alpha$ structural transformation. This would require a special study of the $N_t$ phonon frequency dependence and its changes with the pressure, as was done in this work for the $L$ mode.

## V. CONCLUSION

We have discussed in detail the effect of the vibrational $L$ mode on the structural stability of $\beta$-Zr in a wide range of pressures and temperatures. To this end, the two-mode effective potential of the longitudinal and transverse mode of bcc zirconium with wave vector $\mathbf{k}=2/3(111)$, as well as its changes with pressure and temperature, were successively calculated. It was found that with a reduction in the volume, the energy barrier between the bcc and $\omega$ lattice first decreases in depth, and at volumes below $0.8V_0$, the potential acquires a double-well shape, and the bcc structure becomes energetically preferential.

The effective potentials obtained for different temperatures and volumes were used in solving a set of stochastic differential equations with a thermostat of the white noise type. An analysis of the spectral densities of these modes and their changes under pressure calculated from the autocorrelation velocity functions allowed us to determine the equilibrium temperatures at which $\beta$-Zr remains stable.

The calculated stability region of the Zr $\beta$ phase agrees well with the experimental data available. This suggests that for all pressures considered the main mode, associated with instability of the bcc lattice of zirconium with decreasing temperature, is the longitudinal $L$ mode with wave vector

$\mathbf{k}=2/3(111)$. The particular shape of the equilibrium line between the $\beta$ phase, and the $\alpha$ and $\omega$ phases may be determined by the presence of other anomalous vibrational modes in $\beta$-Zr.

**ACKNOWLEDGMENTS**

The author acknowledges the support from the RFBR Grant No. 04-02-16680.

*Electronic address: tvynew@otf.pti.udm.ru

[1] V. Yu. Trubitsin, preceding paper, Phys. Rev. B **73**, 214302 (2006).
[2] S. Yu. Savrasov and D. Yu. Savrasov, Phys. Rev. B **46**, 12181 (1992).
[3] S. Y. Savrasov, Phys. Rev. B **54**, 16470 (1996).
[4] A. Heiming, W. Petry, J. Trampenau, M. Alba, C. Herzig, and G. Vogl, Phys. Rev. B **40**, 11425 (1989).
[5] A. Heiming, W. Petry, J. Trampenau, M. Alba, C. Herzig, H. R. Schober, and G. Vogl, Phys. Rev. B **43**, 10948 (1991).
[6] S. A. Ostanin, E. I. Salamatov, and V. Yu. Trubitsin, High Press. Res. **17**, 385 (2000).
[7] K.-M. Ho, C. L. Fu, and B. N. Harmon, Phys. Rev. B **29**, 1575 (1984).
[8] G. B. Grad, P. Blaha, J. Luitz, K. Schwarz, A. Fernandez Guillermet, and S. J. Sferco, Phys. Rev. B **62**, 12743 (2000).
[9] E. Yu. Tonkov, *High Pressure Phase Transformations* (Gordon and Breach, Philadelphia, 1992), Vol. 2.
[10] Yu. N. Gornostyrev, M. I. Katsnelson, A. V. Trefilov, and S. V. Tret'jakov, Phys. Rev. B **54**, 3286 (1996).
[11] Y. Chen, C.-L. Fu, K.-M. Ho, and B. N. Harmon, Phys. Rev. B **31**, 6775 (1985).
[12] J. P. Perdew, K. Burke, and M. Ernzerhof, Phys. Rev. Lett. **77**, 3865 (1996).
[13] O. Eriksson, J. M. Wills, and D. Wallace, Phys. Rev. B **46**, 5221 (1992).
[14] H. S. Greenside and E. Helfand, Bell Syst. Tech. J. **60**, 1927 (1981).
[15] S. A. Ostanin and V. Yu. Trubitsin, Phys. Rev. B **57**, 13485 (1998).
[16] Y. Akahama, M. Kobayashi, and H. Kawamura, J. Phys. Soc. Jpn. **59**, 3843 (1990).
[17] Y. Akahama, M. Kobayashi, and H. Kawamura, J. Phys. Soc. Jpn. **60**, 3211 (1991).
[18] A. Jayaraman, W. Klement, and G. C. Kennedy, Phys. Rev. **131**, 644 (1963).
[19] S. A. Ostanin, E. I. Salamatov, and V. Yu. Trubitsin, Phys. Rev. B **57**, 5002 (1998).